Int. J. Electrochem. Sci., 15**(2020)** 8823 – 8836, doi: 10.20964/2020.09.01

International Journal of
ELECTROCHEMICAL
SCIENCE
www.electrochemsci.org

Short Communication

Electrolytic Polishing of Nitinol Based Cardiovascular Stent in NaCl-Ethylene Glycol-Ethanol-Water Electrolyte

Yongqi Wang, Xiuting Wei[*]*, Zhiyong Li, Xiaoyu Sun, Hanqing Liu, Xuemin Jing, Zhikang Gong*

Shandong University of Technology, School of Mechanical Engineering, 266 xincun west road, 255049, Zibo, China
[*]E-mail: wxt@sdut.edu.cn

Received: 6 April 2020 / *Accepted:* 10 June 2020 / *Published:* 10 August 2020

Nitinol (nickel titanium alloy) is well-known as one of the best biocompatible alloys because of its excellent performance. One of the main factors affecting the performance of nitinol cardiovascular stent is their unique surface properties. To improve the surface integrity of these stents, this paper presented an electrolytic polishing method that added ethanol of different concentrations into a glycol - sodium chloride electrolyte to find the optimal electrolyte composition. This paper also investigated the change in surface chemical composition. By plotting the voltage-current density curve and the time-current density curve at various anhydrous ethanol concentrations, the optimal polishing voltage and anhydrous ethanol concentration were determined to be 16 volts and 30%, respectively. According to the time-current density curve, the optimal polishing time was determined to be 20 min, when obtaining the minimum surface roughness (Ra1.837 nm). Furthermore, the surface composition and formation mechanism of the stent after electrolytic polishing were analysed by XPS.

Keywords: Nitinol; Cardiovascular stent; Electrolytic polishing; Roughness; XPS

1. INTRODUCTION

Cardiovascular disease (CVD) refers to the formation of blood clots on the inner wall of blood vessels for various reasons, thereby affecting the pathological phenomena of the heart and blood vessels [1]. In 2016, approximately 17.6 million deaths were attributed to CVD globally [2]. CVD is very common in developed countries and is the leading cause of death due to illness [3]. In Europe, approximately 1.8 million people die each year from CVD, and the EU economy pays approximately 60 billion euros, about one-third of which is paid as direct treatment costs [4]. By 2035, more than 130 million adults in the United States (45.1%) are projected to have some form of CVD, and the total costs of CVD are expected to reach $1.1 trillion [5]. Coronary heart disease (CHD) is the leading cause of death in CVD [4], and the proportion of deaths from CHD in the United States is as high as 43.8% per

year [5]. In the current surgical treatment of CHD, cardiovascular stent implantation is still the main treatment for advanced patients [2, 6]. Therefore, there is a large social need for cardiovascular stents in which a surgeon removes the thrombus by implanting cardiovascular stents with excellent ductility to ensure vascular patency and prevent vascular rupture [7].

Commonly, cardiovascular stents have been made of a nickel-titanium alloy (nitinol), a cobalt-chromium alloy and various types of stainless steel [4]. Nitinol is a shape memory alloy composed of nearly equal atomic Ni and Ti elements [8, 9]; nitinol is martensite at low temperature and austenite at high temperature. The conversion between the two crystal phases gives nitinol unique thermal shape memory properties and superelasticity [10, 11]. Nitinol is one of the best biocompatible alloys because of its excellent performance [12, 13].

The two main factors determining the biocompatibility of nitinol stents are: material-induced host reactions and material degradation in the human environment [14]. In cardiovascular stents, the dissolution of nickel ions can cause problems such as allergies, inflammation [15], and carcinogenicity [16]. The release rate of nickel ion is closely related to the surface quality of the stent, and the higher the corrosion resistance is, the slower the release rate of the nickel ion will be. However, the corrosion resistance of metallic materials is mainly determined by the structure and surface state of the metal [17]. Electrolytic polishing is a very effective process to improve the surface morphology and reduce the roughness of precision micro-metal devices [18]. Therefore, electrolytic polishing of the cardiovascular stent can greatly improve their corrosion resistance.

In recent years, electrolytic polishing has been extensively studied for improving the properties of nitinol. Electrolytic polishing of a nitinol braided stent with an electrolyte configured with acetic acid (79 vol. %) and perchloric acid (21 vol. %) makes the surface of the stent bright and shiny [19]. The electrolytic polishing solution with concentrated phosphoric acid, concentrated sulfuric acid and deionized water in a certain proportion has significantly improved the surface appearance and corrosion resistance of the alloy after polishing [20]. The nitinol is polished in an electrolyte containing a small amount of water in methanol and sulfuric acid to obtain small surface roughness and the desired current efficiency [21]. Using an electrolyte mixed with sulfuric acid and methanol, an ideal nitinol sample with a bright surface and low surface roughness was obtained at 298K [22]. Nitinol surfaces with uniform deformation and high corrosion resistance were obtained in an electrolyte solution of hydrofluoric acid, sulfuric acid and ethylene glycol [23].

All these studies suggest that the current electrolytic polishing solutions for nitinol mainly use acidic electrolytes such as sulfuric acid, hydrofluoric acid, perchloric acid and nitric acid [14, 24]. The advantage of the acidic electrolyte is that the polishing efficiency is high and the development is relatively mature; however, the disadvantages are also obvious. The electrolytic polishing process is prone to excessive electrolytic polishing, the subsequent process is complicated, the cost is high, and there are great hidden safety risks. To avoid the danger and difficulty of acidic electrolytes and reduce environmental damage, the aims of this study were as follows: (1) to propose a method of electrolytic polishing of Nitinol cardiovascular stents using an environmentally friendly electrolyte, specifically to study the effect of adding different ethanol concentrations in the glycol-sodium chloride electrolyte, (2) to find the best composition and concentration of electrolyte and polishing voltage, and (3) to investigate the chemical composition changes on the surface and changes in the surface integrity. Surface roughness

and surface topography were examined using an optical profiler (MicroXAM-100), atomic force microscopy (AFM) and a field emission environment scanning electron microscope (FE-SEM). X-ray photoelectron spectroscopy (XPS) was used to analyse the surface composition and formation mechanism after electrolytic polishing.

2. EXPERIMENTAL

A cardiovascular stent made of nitinol (Ni56.14at.%) material after laser cutting was used as a sample, with an outer diameter of 2.6 mm, wall thickness of 0.2 mm, and length of 13 mm. To eliminate impurities, the stent was first mechanically polished with #500 SiC paper and then treated for 5 minutes in an ultrasonic cleaner using acetone as a cleaning agent. Commercially available ethylene glycol (99% pure with 1 wt% of water) was mixed with sodium chloride to form a 1 mol/L sodium chloride-ethylene glycol electrolyte solution. In addition, anhydrous ethanol (>99.9%) was added to the electrolyte solution at various concentration (5, 10, 20, 30 and 35 vol. %). The DC power supply voltage range is 4-32 V. For voltages of 6-18 V, the step is 1 V, while the other voltage step is 2V. The polishing time is 10-50 min. In 10-30 min, the step is 5 min, while in 30-50 min, the step is 10 min. Table 1 summarizes the specific experimental parameters and labelling of the various electrolyte solutions.

Table 1. Electrolytic polishing specific experimental parameters

Voltage(V)	4, 6-18 (Step size 1), 20-32 (Step size 2)
Anode	Nitinol cardiovascular stent
Electrolyte	5, 10, 20, 30, 35(vol. %) Anhydrous ethanol; 1 mol/L NaCl; 99.0% Ethylene glycol
Cathode	304-grade stainless steel ring
Temperature	20 °C
Time(min)	10, 15, 20, 25, 30, 40, 50

Figure 1 shows a schematic diagram of the experimental equipment. The electrolyte solution temperature was controlled by using a constant temperature environment with a chiller at 20 °C. A beaker with a capacity of 1000 ml was used as the electrolyte container. A sheet of 304-grade stainless steel (STS304) was used as the counter electrode, which was made into a ring with a diameter of 52.6 mm and a height of 20 mm. The treated nitinol cardiovascular stent was used as the anode. The distance between the anode and cathode is 25 mm. The cardiovascular stent was clamped by a silicone hollow tube with an outer diameter of 6.6 mm, a wall thickness of 2.3 mm and a height of 6 mm. The hollow stent is interference fit on the plastic rack. A magnetic stirrer (Shanghai Hu Xi 85-2WS, Shanghai Hu Xi Industrial Co., Ltd., China) stirs the solution and takes the temperature. The stirring rate was maintained at 800 rpm and the temperature sensor was inserted into the electrolyte solution.

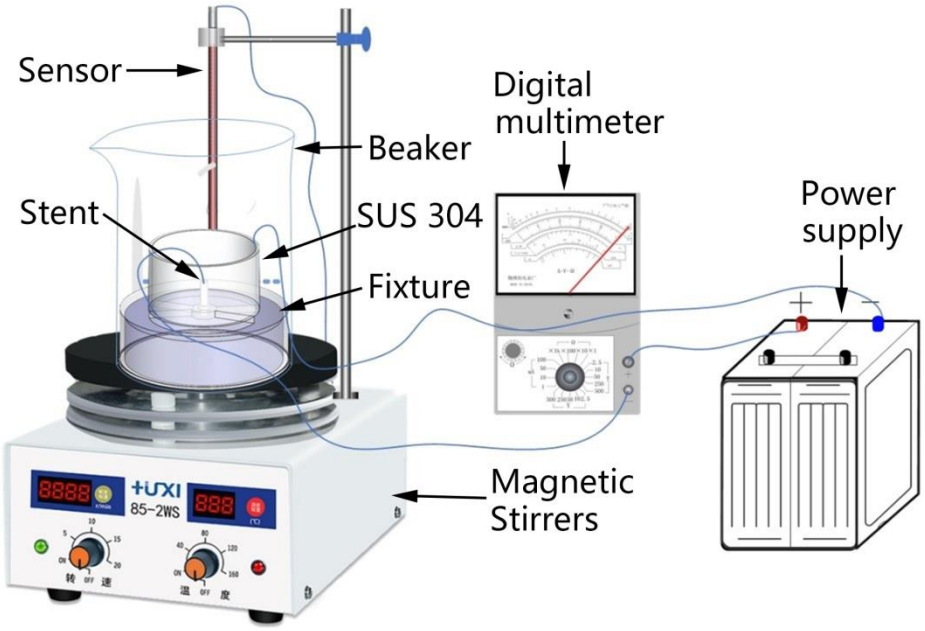

Figure 1. Schematic diagram of the experimental equipment

The voltage-current density curve and the time-current density curve under diverse conditions were plotted with a digital multimeter (PROVA 901, Taiyi Electronics Co., Ltd., Taiwan, China). The polished stent was washed in an ultrasonic cleaner for 3-5 min. The surface morphology and chemical bonding environment were investigated by field emission scanning electron microscopy (FE-SEM, FEI Quanta 250, America) and X-ray photoelectron spectroscopy (XPS, AXIS SUPRA, Al Kα, 1486.6eV, UK). The XPS analysis area was 750μm^2 and the X-ray energy was 15kV. Furthermore, the surface roughness (Ra) and 3D images were obtained with an optical profiler (MicroXAM-100, Shanghai Weiner Metrology Technology Co., Ltd., China) and an atomic force microscope (AFM, nt-mdt solver scanning probe microscope BL222, Russia).

3. RESULTS AND DISCUSSION

3.1 Best experimental parameters

Figure 2 shows the voltage-current density curve used to find the electrolytic polishing range of the stent according to the anhydrous ethanol concentration in the electrolyte solution in view of the fact that each system (distance between poles, electrolyte) was not identical. Region I (4-10 V) is a current density that increases rapidly with increasing voltage, and region II (10-14 V) is a voltage increase with a slight decrease in current density. Corrosion reactions occur in regions I and II. The surface colour of the stents is partly black, and the polishing quality is not ideal. The current density of region III (14-18 V) is smooth because its changes are relatively small; therefore, the polishing effect is the best. Region IV (18 V-32 V) shows a linear increase in current density and voltage, and the surface mainly undergoes

pitting reaction with poor surface quality. Therefore, the optimum polishing region is III (14-18 V), which is economical and guarantees good polishing quality. For the optimal balance between the electrical power and electrolytic polishing quality, a constant 16 V was applied for the rest of the study, unless stated otherwise.

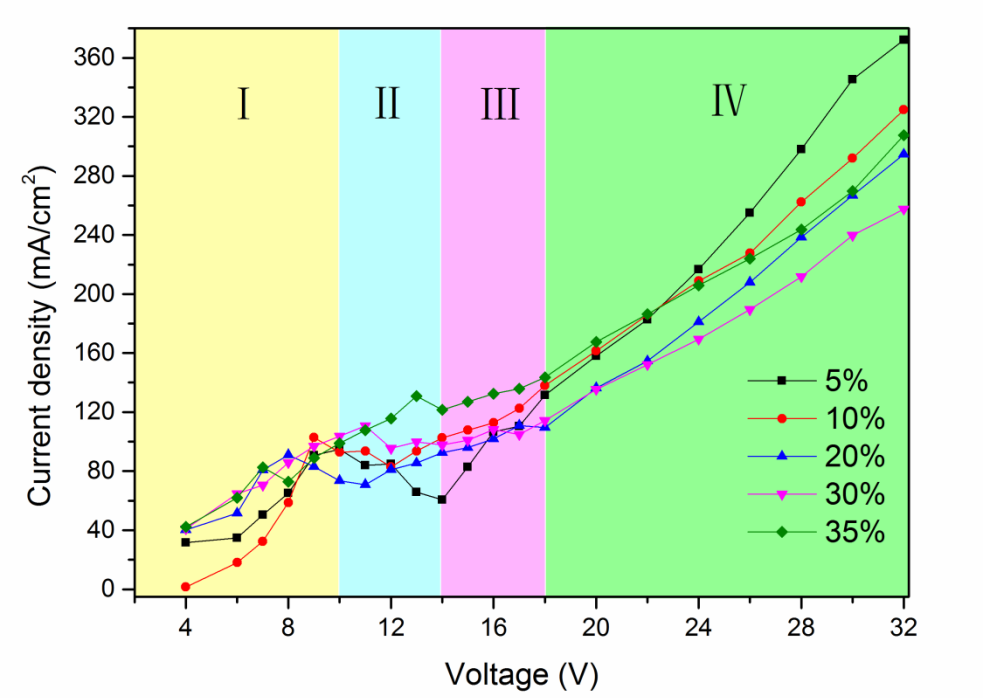

Figure 2. Voltage-current density curve obtained for the electrochemical reaction of a nitinol cardiovascular stent as a function of the anhydrous ethanol concentration in a sodium chloride-ethylene glycol electrolyte solution.

Figure 3 shows the time-current density curve of nitinol cardiovascular stents at various ethanol concentrations. The current density is gradually reduced with the addition of 5%-30% absolute ethanol with the prolongation of polishing time, indicating that the stent surface is mainly for the removal of bulk metal, and the pitting reaction occurs less. However, the current density of the stent slowly increases with time when the absolute ethanol concentration reaches 35%, indicating that an accelerated pitting reaction occurs on the surface of the cardiovascular stent over time. According to the current density value in Figure 3, the first 10, 15, 20, 25, 30, 40 and 50 min are sampled, and the variance is calculated. The absolute ethanol concentration-variance box plot is shown in Figure 4.The figure shows that the optimum volume fraction of anhydrous ethanol is 30%, indicating that the current density stability is the best at this time. Therefore, the concentration of anhydrous ethanol added is preferably 30%.

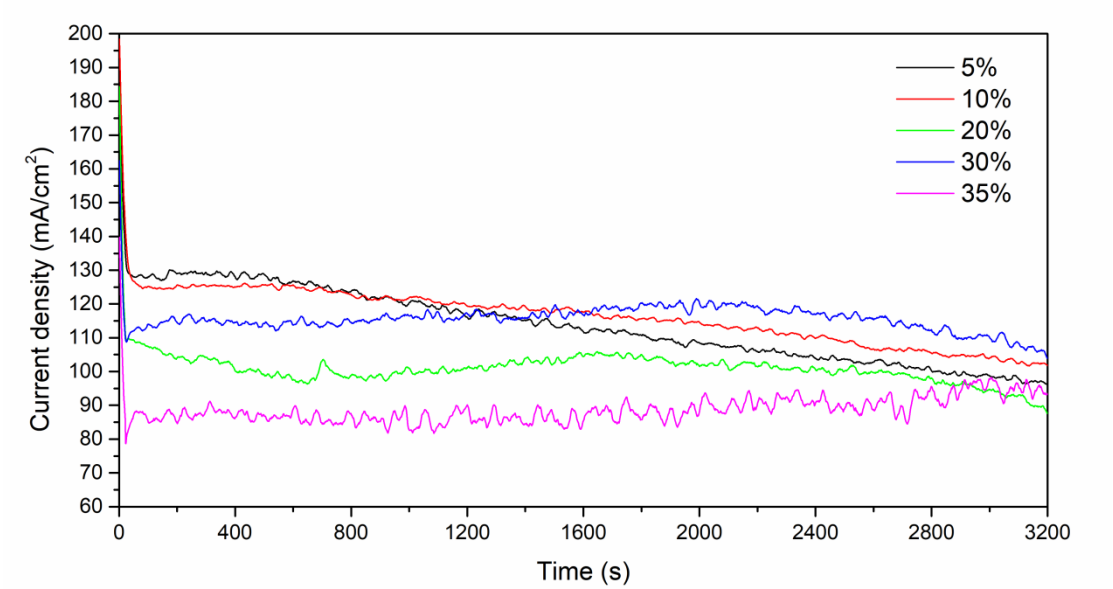

Figure 3. Time-current density curve obtained during the electrolytic polishing of the nitinol cardiovascular stent with a voltage of 16 V in a sodium chloride-ethylene glycol electrolyte solution containing various concentrations of anhydrous ethanol.

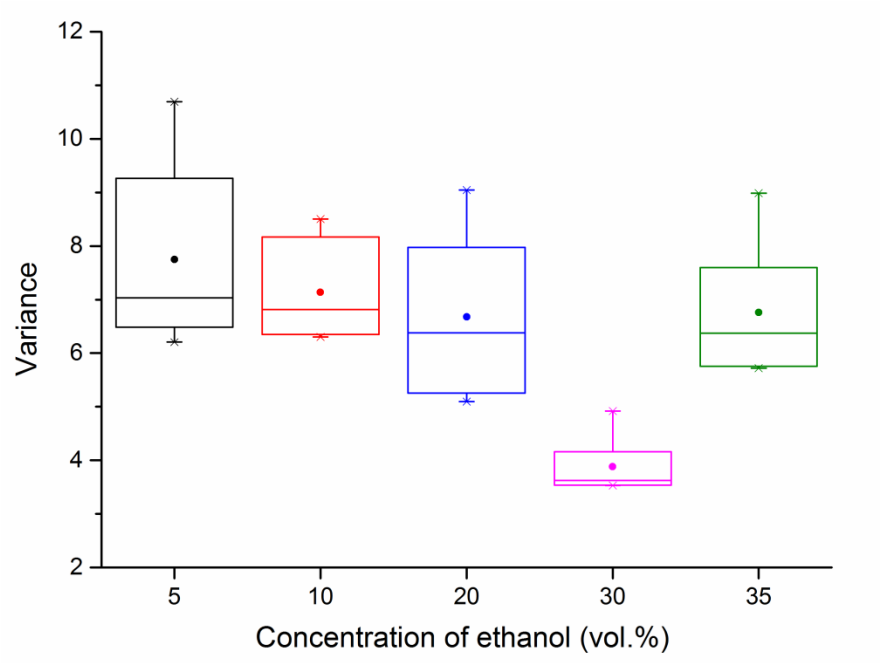

Figure 4. Anhydrous ethanol concentration-variance box plot obtained by calculating the variance of the current density of the seven electrolytic polishing time periods based on the time-current density curve of Figure 3.

Figure 5 shows a box plot of the surface roughness-polishing time for a 30% absolute ethanol concentration. The surface roughness of the stent is measured at different stent locations after polishing. When polished for 20 min, the median and minimum roughness of the roughness values is optimal.

Compared with other electrolytic polishing times, the value is more stable. Compared with the currently known lowest roughness (Ra 22.29 nm), the lowest roughness in this study is 1.837 nm, which greatly reduces the roughness of the stent [25] and indicates that the surface quality of the stent obtained by this method is relatively good.

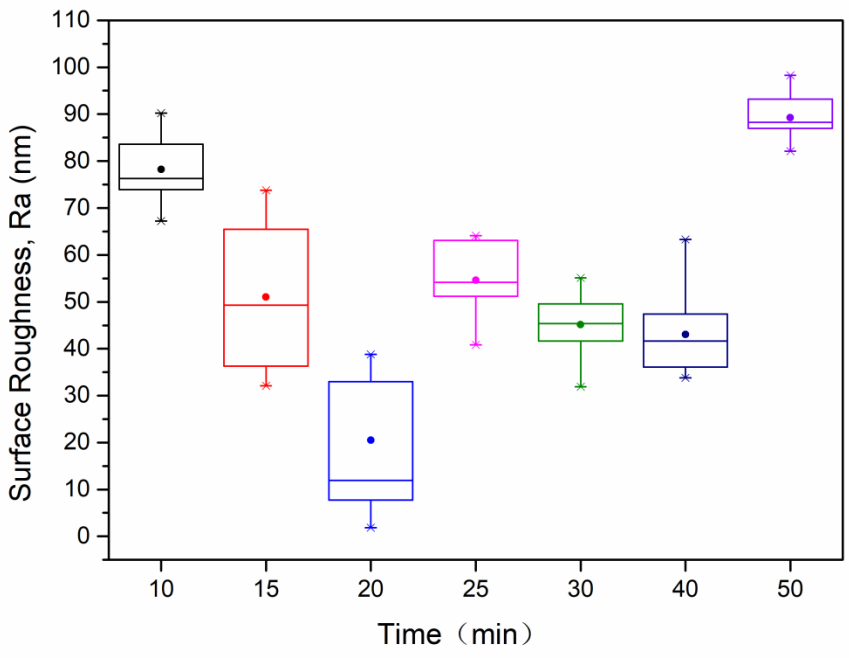

Figure 5. Electrolytic polishing time-Ra values box plot of nitinol cardiovascular stent in sodium chloride-glycol electrolyte solution with 30% anhydrous ethanol at 16 V.

3.2. Surface study and composition analysis

3.2.1 Surface study: AFM, FE-SEM, and Optical Images

Figure 6 shows a 3D AFM image of the surface of a stent electropolished in a sodium chloride-ethylene glycol electrolyte solution configured with 30% ethanol at a voltage of 16 V for 10-40 min. The surface of the stent after electrolysis for 30 min and 40 min was similar, but the maximum height of the stent surface after electrolytic polishing for 20 min was below 50 nm, and the surface was the smoothest.

Furthermore, Figure 7 shows an FE-SEM image of the stent at 0, 20, and 50 min of polishing. A large amount of slag, microcracks and scratches are present at the surface of the stent treated by electrolytic polishing for 0 min in Figure 7a. As shown in Figure 7b, a smooth and slag-free surface was produced on the cardiovascular stent after electrolytic polishing for 20 min. In Figure 7c, obvious grain boundaries and pitting pits appeared on the surface of the stent after electrolysis for 50 minutes. The FE-SEM images correspond well with the results measured by the optical profilometer, indicating that the optimal time for electrolytic polishing of a nitinol cardiovascular stent is 20 min.

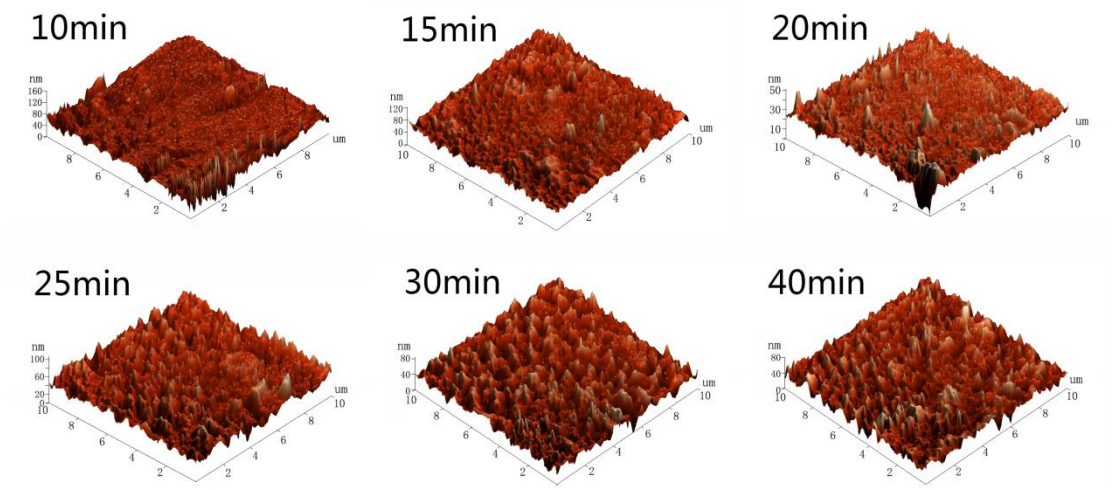

Figure 6. 3D images of 10 × 10 μm areas of the stent surface.

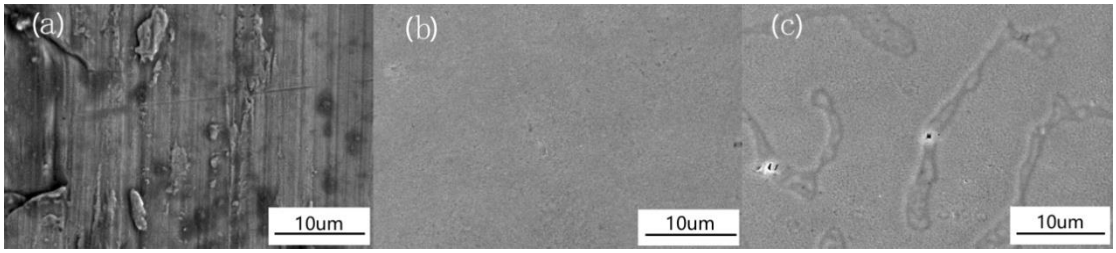

Figure 7. Surface morphology of nitinol cardiovascular stents by FE-SEM in a sodium chloride-glycol electrolyte solution with 30% anhydrous ethanol at 16 V: (a) unelectrolyzed stent; (b) electrolytic polishing 20 min; (c) electrolytic polishing 50 min.

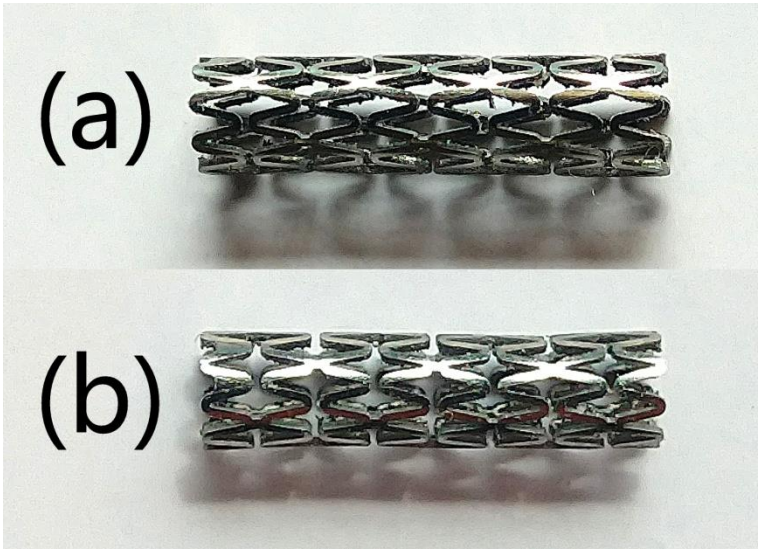

Figure 8. Optical images of the surfaces of the nitinol cardiovascular stent: (a) unelectrolyzed stent; (b) stent electrolyzed in a sodium chloride-glycol electrolyte solution of *30*% ethanol at *16* V for 20 minutes.

Figure 8 shows the unelectrolyzed stent and the stent polished under the optimal parameters. Prior to electrolytic polishing, the stent surface was covered with slag and a black oxide produced by laser processing. It can be seen that the electrolytic polishing process removed surface slag and thermal oxide, leading to a bright and shiny surface.

3.2.2 Composition analysis

The surface chemical composition of different samples was analysed by XPS. Survey scans were carried out between 0 and 1200eV at 80eV constant pass energy on the unelectrolyzed stent, as shown in Figure 9(a). The image shows that the main components of the stent surface are C, Ti, O and Ni. For the stent electrolytic polished for 20 min, survey scans were carried out between 0 and 1200eV at 80eV constant pass energy, as shown in Figure 9(b). The figure shows that after 20 minutes of electrolytic polishing, the element types of the stent change little, but the Ti and O contents increase significantly. High-resolution scans were obtained stent for the Ti 2p region using 40eV pass energy. As shown in Figure 9(c), on the surface of the unelectrolyzed stent, only 458.0eV had a main peak at the binding energy, corresponding to TiO_2 $2p^{3/2}$. As shown in Figure 9(d), when electrolytic polishing for 20 min, the two main peaks were located at 459.0eV and 454.3eV, corresponding to TiO_2 $2p^{3/2}$ and Ti $2p^{3/2}$, respectively. In addition, there are two sub-strong peaks corresponding to $TiCl_4$ $2p^{3/2}$ (459.8eV) and TiO_2 $2p^{1/2}$ (464.7eV).

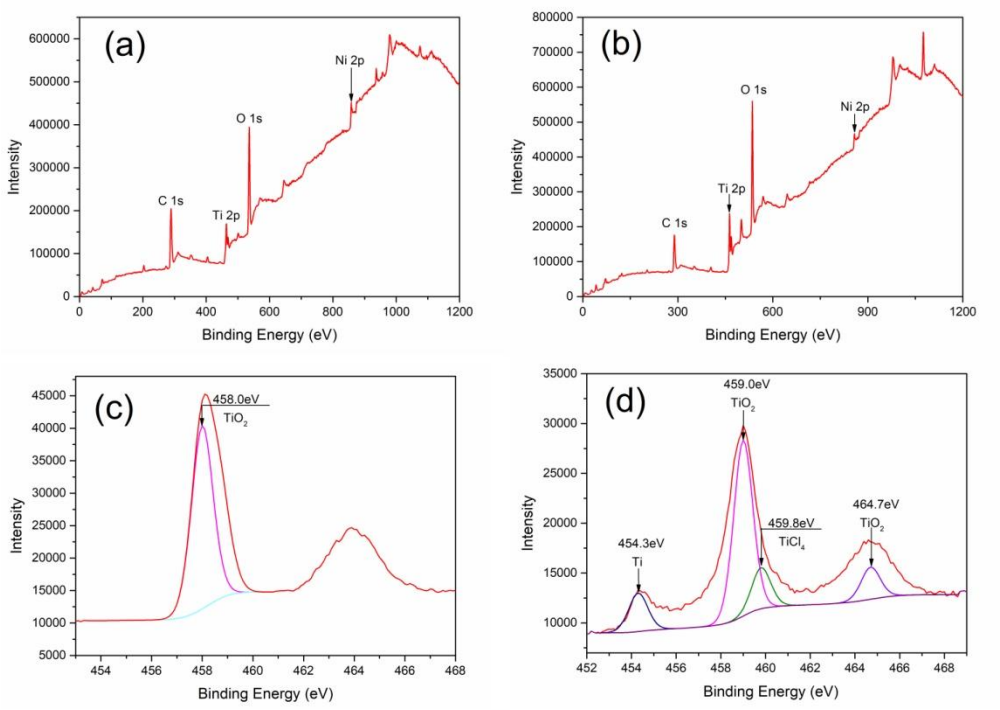

Figure 9. XPS spectra of nitinol cardiovascular stents: (a) 0 and 1200 eV scanning over a wide range of unelectrolyzed stents; (b) 0 and 1200 eV scanning over a wide range of electrolytic polishing 20 min stents; (c) Ti 2p XPS results of unelectrolyzed stents; (d) Ti 2p XPS results of electrolytic polishing 20 min stents.

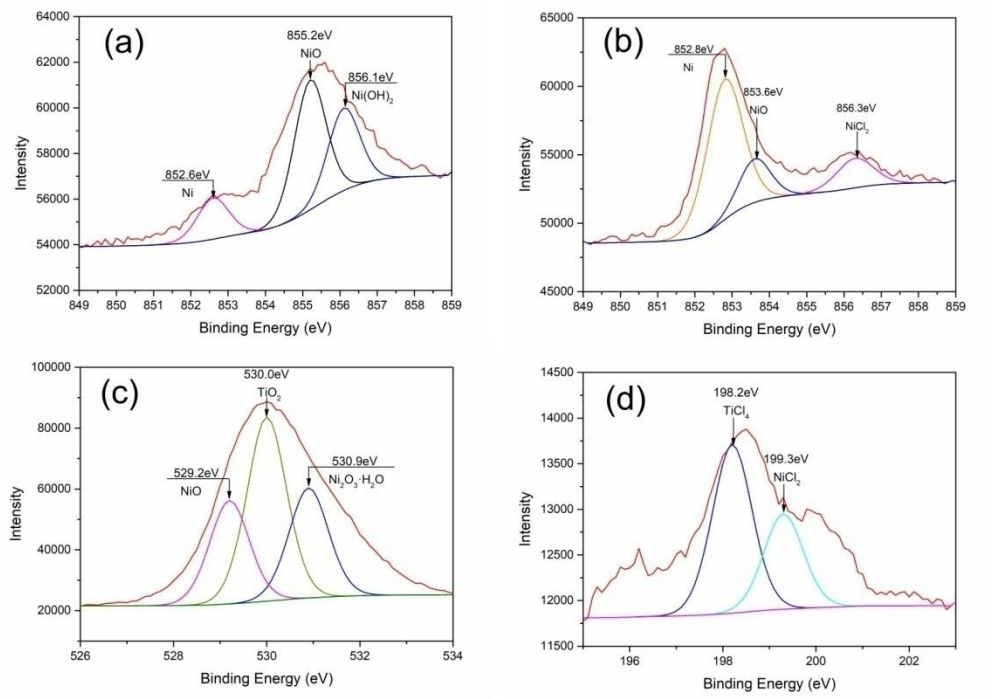

Figure 10. XPS spectra of nitinol cardiovascular stents: (a) Ni 2p XPS results of unelectrolyzed stents; (b) Ni 2p XPS results of electrolytic polishing 20 min stents; (c) O 1s XPS results of unelectrolyzed stents; (d) Cl 2p XPS results of electrolytic polishing 20 min stents.

As shown in Figure 10, high resolution scans were obtained for the Ni 2p, O 1s and Cl 2p region using 40eV pass energy. As shown in Figure 10(a), on the surface of the unelectrolyzed stent, a main peak was located at 855.2eV, corresponding to NiO $2p^{3/2}$. In addition, there are two sub-strong peaks corresponding to $Ni(OH)_2$ $2p^{3/2}$ (856.1eV) and Ni $2p^{3/2}$ (852.6eV). As shown in Figure 10(b), electrolytic polishing for 20 min, one main peak was located at 852.8eV, corresponding to Ni $2p^{3/2}$. In addition, there are two sub-strong peaks corresponding to NiO $2p^{3/2}$ (853.6eV) and $NiCl_2$ $2p^{3/2}$ (856.3eV). As seen from Figures 9 and 10, the electron binding energy of nickel and titanium changed significantly after electrolytic polishing. Combined with high resolution scanning of O 1s for the unelectrolyzed stent and of Cl 2p electrolytic polishing for 20 min, the surface components for the unelectrolyzed stent and electrolytic polishing for 20 min were calculated respectively. Due to the presence of oxygen in the air, high resolution scanning of O 1s was not performed for 20 minutes, and Cl 2p was less affected by the environment. The results of the high-resolution scan using Cl 2p are more accurate.

The analysis results of atom% are summarized in Table 2, which shows that the compound on the surface of the unelectrolyzed stent consists mainly of TiO_2, NiO and Ni_2O_3•H_2O. The ratio of titanium atoms to nickel atoms is 0.52 before electrolysis and reaches 1.26 at 20 minutes. TiO_2 increased from 39.7% to 46.03%. The energy dispersive spectrometer scan of the stent again reached the same conclusion.The decrease in nickel content may be the reason for the preferential consumption of nickel atoms during the electrolytic polishing process [26, 27].

Table 2. The surface composition of nitinol cardiovascular stent was determined by XPS at 16 V electrolysis for 0 and 20 min.

Time	Ni	Ti	NiO	TiO_2	$NiCl_2$	$TiCl_4$	$Ni_2O_3{\cdot}H_2O$	Else
0min	5.95%	0	22.34%	39.7%	0	0	23.78%	8.23%
20 min	29.75%	4.63%	12.05%	46.03%	2.51%	5.03%	0	0

During the electrolytic polishing process, Ni^{2+} and Ti^{4+} ions at anode react with Cl^- ions in the electrolyte solution and produce nickel dichloride ($NiCl_2$) and titanium tetrachloride ($TiCl_4$), as shown in equation (1) and equation (2), respectively:

$$Ni^{4+} + 2Cl^- \rightarrow NiCl_2(l) \quad (1)$$

$$Ti^{4+} + 4Cl^- \rightarrow TiCl_4(l) \quad (2)$$

$TiCl_4$ is a very sticky liquid attached to the surface of the anode and forms a $TiCl_4$ film. $NiCl_2$ is easily soluble in water and ethanol, and most of the $NiCl_2$ dissolves into the electrolyte. Although water was not added to the electrolyte solution in this research, in addition to the vapor absorbed from the atmosphere, water molecules were always inevitable in the ethanol and ethylene glycol solutions. Therefore, $NiCl_2$ and $TiCl_4$ react with water（H_2O）and produce nickel monoxide (NiO) and titanium dioxide (TiO_2), as shown in equation (3) and equation (4), respectively:

$$TiCl_4(l) + 2H_2O \rightarrow TiO_2(s) + 4H^+ + 4Cl^- \quad (3)$$

$$NiCl_2(l) + H_2O \rightarrow NiO(s) + 2H^+ + 2Cl^- \quad (4)$$

The TiO_2 and NiO produced by the reaction are chemically stable. TiO_2 has a strong binding force on the surface of the stent, and its existence is the root cause of improved corrosion resistance and biocompatibility of the stents.

3.3 Comparison with similar results

In the literature, there are practically no reports concerning electrolytic polishing of nitinol based cardiovascular stent. This paper reports for the first time the electrolytic polishing of cardiovascular stents using an environmentally friendly electrolyte based on nickel-titanium alloy. The few papers examining Nitinol alloy stents, such as references [28] and [29], use nitric acid and perchloric acid electrolyte. Furthermore, previous research did not study the changes in surface chemical composition. In contrast, ample data concerning the electrolytic polishing of titanium and its alloys have been published. References [30], [31], [32] and [33] use mainly sulfuric acid as the electrolyte; the solvent treatment after polishing is more complicated and environmental requirements are not met. In addition, using the electrolytic polishing parameters of this study, the surface roughness can be reduced to 1.837 nm, which is also a breakthrough. See Table 3 for specific comparison.

Table 3. Compared with similar discussion and results

No.	Research object	Electrolyte	Roughness (nm)	Chemical composition on surface	Ref.
1	NiTi alloy Stents	n-butanol, nitric acid	22.29	N.A.	[28]
2	NiTi braided stents	acetic acid and perchloric acid	N.A.	N.A.	[29]
3	NiTi shape memory alloys plate	sulfuric acid, hydrofluoric acid and ethylene glycol	9.5	exist	[30]
4	NiTi shape memory alloys plate	phosphoric acid, sulfuric acid and distilled water	N.A.	N.A.	[31]
5	NiTi shape memory alloys plate	sulfuric acid and methanol	Over 20	N.A.	[32]
6	NiTi shape memory alloys plate	sulfuric acid and methanol	32	exist	[33]
7	Nitinol based cardiovascular stent	NaCl-ethylene glycol-ethanol-water electrolyte	1.837	exist	This work

4. CONCLUSIONS

This paper presents a method for electrolytic polishing of Nitinol cardiovascular stents using an environmentally friendly electrolyte. Different concentrations of ethanol were added into a NaCl-ethylene glycol electrolyte for electrolytic polishing of nitinol cardiovascular stents at room temperature. After polishing, the surface properties were greatly improved. The optimal electrolyte composition and concentration and the surface chemical composition changes were studied through experiments. The main conclusions are as follows:

1. At room temperature, using a voltage of 16 V, adding 30% anhydrous ethanol and electrolytic polishing for 20 min, an ideal stent surface can be obtained.

2. Under these parameters, the surface quality of the stent sample was significantly improved from an average Ra 1.2μm to a minimum Ra 1.837 nm which was better than the known minimum roughness.

3. After electrolysis, the TiO2 content is significantly increased, which improves the corrosion resistance of the cardiovascular stent.

4. The polishing method not only solves the safety hazard and complicated electrolyte treatment problems but also has the advantages of safety, environmental protection, simple processing and good surface quality.

ACKNOWLEDGEMENTS
This study was supported by the NSFC (Grant No.51775321) and Shandong Education Department about key research and development plan (public welfare) project of Shandong Province in China (Grant No. 2017GGX30116).The authors declare that they have no conflict of interest.

References

1. L. Neelakantan, M. Valtiner, G. Eggeler, and A.W. Hassel., *Mater. Chem. Phys.*, 220 (2018) 35.
2. E.J. Benjamin, P. Muntner, M.S. Bittencourt, B.M. Kissela and C.W. Callaway, *J. Am. Heart Assoc.*, 139 (2019) 56.
3. F. Boccafoschi, L. Fusaro, M. Cannas, and L. Djousse, *Appl. Surf. Sci.,* 421 (2018) 25.
4. M. Cormick, M. Chamberlain, S. Cheng and N. Delling, *J. Colloid Interf. Sci.,* 517 (2018) 51.
5. E.J. Benjamin, S. Virani, C.W. Elkind, L.C. Jordan, S. Khan, and M. Fornage, *J. Ind. Eng. Chem.*, 54 (2019) 353.
6. C. Quint, M. Arief, A. Muto, A. Dardik, and L.E. Niklason, *J. VASC. SURG*, 55 (2012) 790.
7. K. Permana, A.Shuib, D. Ariwahjoedi, and W. Kwan, *J. Mol. Liq.,* 89 (2013) 13.
8. W. Buehler, T. Lackland, T. Lewis , and H. Lichtman, *Trans. Am. Soc. Med*, 55 (1962) 269.
9. G. Kauffman, B. Mayo, T. Longenecker and M.S. Loop, *Adv. Manuf. Technol.*, 591 (1997) 16.
10. M. Szold, J. Patscheider, and L. Lutsey, *Surf. Coat. Technol*, 20 (2016) 143.
11. X. Huang, G.J. Ackland, and K.M. Rabe , *Nat. Mater.*, 20 (2013) 317.
12. A. Bhardwaj, A.K. Gupta, S.K. Padisala, and K. Poluri, *Mater. Sci. Eng., C,* 102 (2019) 730.
13. D. Stoeckel, A. Pelton, and T, Duerig, *Corros. Sci.* 14 (2004) 292.
14. W. Simka, M. Kaczmarek, A. Baron-Wiecheć, G. Nawrat, J. Marciniak, and J. Żak, , *Electrochim. Acta*, 55 (2010) 2437.
15. J.C. Wataha, N. Dell, L. Singh, B. Ghazi, M. Whitford, and G. Lockwood, *J. Biomed. Mater. Res. Part A*, 58 (2001) 537.
16. Y. Okazaki, and E. Gotoh, *Corros. Sci.*, 50 (2008) 3429.
17. R. W. Poon, J.P. Liu, X. Chung, C.Y. Chu, P. K. Yeung, and K. Cheung, *Nucl. Instrum. Methods Phys. Res., Sect. B*, 237 (2005), 411.
18. Z. Zhang, Z. Shi, Y. Du, Z. Yu, and L. Guo, *Appl. Surf. Sci.*, 427 (2018) 409.
19. E. Kassab, A. Marquardt, L. Neelakantan, M. Frotscher, and F. Schreiber, *J. Mol. Liq.,* 45 (2014) 920.
20. X. Xu, T. Zhang, Z.Y. Ling, X. Sheng and M. Liu, *J. Mol. Liq.,* 126 (2017) 189.
21. K. Fushimi, M. Stratmann, and A.W Hassel, *Electrochim. Acta.,* 52 (2006) 1290.
22. L. Neelakantan, A. Hassel, *Electrochim. Acta,* 53 (2007) 915.
23. W. Simka, M. Kaczmarek, A. Baron-Wiecheć, Nawrat, and J. Baulak, *Electrochim. Acta,* 55 (2010) 2437.
24. T. Nishiura, K. Hayashi, and M. Nishida, *Mater. Sci. Eng., A*, 481 (2008) 446.
25. J. Kim, J.K. Park, H.K. Kim, A.R. Unnithan, and C.S. Kim, *J. Biomed. Mater. Res.*, 17 (2017) 2333.
26. B. Thierry, M. Tabrizian, C. Trepanier, O. Savadogo, and L.H. Yahia, *J. Biomed. Mater. Res. Part B*, 51 (2000) 685.
27. D.A. Armitage, and D.M. Grant, *Mater. Sci. Eng., A*, 349 (2003) 89.

28. J. Kim, J.K. Park, H.K. Kim, A.R. Unnithan, and C.S. Kim, *J. Biomed. Mater. Res.*, 17 (2017) 2333.
29. E. Kassab, A. Marquardt, L. Neelakantan, M. Frotscher, F. Schreiber, and T. Gries,G, *J. Ind. Eng. Chem.*, 45 (2014) 920.
30. W. Simka, M. Kaczmarek, A. Baron-Wieche, G. Nawrat, J. Marciniak, and J. Żak, *Electrochim. Acta*, 55 (2010) 2437.
31. G. B. Pound, and W. Tsao, *J. Biomed. Mater. Res. Part B.* 4 (2018) 106.
32. K. Fushimi, M. Stratmann, and A.W Hassel, *Electrochim. Acta*, 45 (2016) 127.
33. L. Neelakantan, M. Valtiner, G. Eggeler, and A.W. Hassel, *Phys. Status Solidi A*, 4 (2016) 207.